

Optical Dichroism by Nonlinear Excitations in Graphene Nanoribbons

C. E. Cordeiro¹, A. Delfino¹, T. Frederico², O. Oliveira^{2,3} and W. de Paula⁴

¹*Instituto de Física, Universidade Federal Fluminense, 24210-3400- Niterói - RJ, Brazil*

²*Departamento de Física, Instituto Tecnológico de Aeronáutica, 12.228-900, São José dos Campos, SP, Brazil*

³*Departamento de Física, Universidade de Coimbra, 3004-516 Coimbra, Portugal*

⁴*Departamento de Física, Universidade Federal de São Carlos, 13565-905 São Carlos, SP, Brazil*

(Dated: July 2, 2018)

The honeycomb carbon structure of graphene and nanotubes has a dynamics which can give rise to a spectrum. This can be excited via the interaction with an external electromagnetic field. In this work, non-linear waves on graphene and nanotubes associated with the carbon structure are investigated using a gauge model. Typical energies are estimated and their scaling with the nanoribbon width is investigated. Furthermore, the soliton-photon interaction depends on the incident photon polarization. In particular, we find that the nanoribbon is transparent when the polarization is along the largest length. Relying on the scaling with the width, we suggest a way to experimentally identify the soliton waves in nanoribbons.

PACS numbers: 71.10.-w,72.80.Vp,11.10.Kk

I. INTRODUCTION AND MOTIVATION

The physics of nano-materials has been the subject of intense investigation in the past years. In particular, graphene and nanotubes¹⁻⁵ have been studied due to its potential technological applications and its peculiar electronic properties, see^{6,7}.

A popular approach to understand graphene and nanotubes is to use tight-binding or Hubbard like models to describe the behavior of electrons and holes. Despite its success, these type of models do not take into account the dynamics of the honeycomb array of carbon atoms. Therefore, dynamical effects connected directly with the carbon structure are not taken into account by those type of models.

A chiral gauge model for graphene was suggested in⁸. In⁹ it was studied its generalisation to include other gauge groups, not necessarily chiral invariant. The models are able to accommodate the main features of the electronic properties in graphene, like the creation of mass gaps or quantum Hall effects, and parameterizes the dynamics of the carbon background structure via a charged scalar field φ and spin one fields A_μ . The model allows to go beyond the electronic properties and to investigate phenomena which are related with the dynamics of the carbon crystal structure. Indeed, the authors explored the non-linear dynamics of φ and A_μ to compute mass gaps, to derive finite energy vortex solutions, which can lead to flux quantisation and Aharonov-Bohm effects (see e.g.¹⁰ and references therein) and to check that the gauge theory is compatible with the experimentally observed electronic quantum Hall effect. Furthermore, the fermionic zero modes associated to the finite energy vortex configurations⁹ are solutions of a one dimensional Schrödinger-like equation with a scale invariant $1/z^2$ potential¹¹. Certainly, the theory can accommodate other phenomena not explored so far and, in particular, phenomena whose dynamics is linked with the honeycomb array of carbon atoms.

The complex scalar field φ and A_μ model the dynamics of the carbon crystal structure, on top of which electrons and holes live. Certainly, the electronic properties of graphene are sensitive to the φ and A_μ configurations. Changing the configuration of the bosonic fields, the electrical and thermal transports properties associated with the fermionic degrees of freedom change accordingly. For example, phonons are associated with fluctuations of φ and A_μ around a given configuration and contribute to the graphene specific heat. Then, the investigation of the thermal properties of graphene can help understanding the bosonic part of the gauge model. On the other hand, the scalar field φ being a charged field, it couples directly to the electromagnetic field C_μ and can contribute to the graphene optical properties. Therefore, within the gauge model of^{8,9}, it is of paramount importance to understand how the bosonic degrees of freedom can be excited via the coupling with an external field. If one is able to control the φ and A_μ configurations by coupling with external fields, one can achieve a better control of graphene and, in general, nano-materials properties.

From the pure field theory point of view, φ couples directly to the fermions and, for example, can trigger the generation of a fermionic mass gap. Given that φ is a dynamical field, the model allows us to define regions where the mass gap vanishes, while in other regions the fermions acquire a finite mass with the corresponding decreasing of its mobility, i.e. from the point of view of the gauge model the mass gap is, itself, a dynamical quantity. One would like to understand what type of φ configurations are allowed and how they impact on the electronic properties.

The self-couplings of φ allow for solitonic solutions of the fields equations. In this work, we will use the term solitonic solution to describe any solution of the non-linear differential equation of motion for φ . The field fluctuations around the soliton can give rise to phonons with new types of dispersion relations. One expects contributions to the optical and thermal properties of graphene

coming from the solitonic waves. Furthermore, φ has a non-vanishing electric charge and the non-linear waves couples with an external electromagnetic field. This coupling opens the possibility of generating these non-linear modes by exciting graphene with a laser or a properly tuned electromagnetic field.

The gauge model suggested in⁹ is an effective quantum field theory for the dynamics of a 2+1 dimensional system. In principle, it can be applied to any 2D nano-materials, other than graphene. In this work we will also consider nanotubes. From the point of view of the gauge theory, the main difference between the two systems is the geometry of the two carbon based materials. If graphene is associated with a 2D flat sheet, a nanotube is a two dimensional material having the same type of unit cell but with a cylindrical geometry.

In this paper, we investigate the classical solutions of the non-linear bosonic equations of motion of the gauge model⁹ for graphene and nanotubes. Besides computing explicitly non-linear configurations for φ and A_μ , we also discuss how these nonlinear modes couple with an external electromagnetic field. In particular, we find that the coupling between the nonlinear modes and the photon field displays dichroism, i.e. the ability to absorb light depends on the polarization state of the incoming photon. Dichroism with a strong absorption anisotropy from the electronic intraband transitions requiring a finite chemical potential was investigated in¹⁷. For these two cases, the pattern of the coupling with the polarization of the photon is similar, i.e. the graphene nanoribbon is transparent when the polarization is along the largest length of the carbon material, but also the energy range where dichroism is expected to be seen is in the far infrared and terahertz frequencies. If the intraband transition requires a non-vanishing chemical potential μ to generate dichroism, the coupling with the nonlinear waves is independent of μ . This observation enables to experimentally distinguish between the two mechanisms.

The paper is organized as follows. In section II we review the gauge model. The coupling with an external electromagnetic field is discussed, the equations of motion and the Hamiltonian for the gauge model are derived. In section III the solitonic solutions of the classical equations are discussed in the present context. In section IV we investigate the soliton-photon transition amplitude and decay rate. Finally, in section V we resume and conclude.

II. GAUGE MODEL FOR GRAPHENE AND NANOTUBES

For completeness, in this section we resume the main features of the gauge model described in⁹. The interested reader should look at the cited paper for a detailed discussion.

The model describes electrons and holes via a Dirac equation in two dimensions using a four component

spinor

$$\Psi = \begin{pmatrix} \psi_+^b \\ \psi_+^a \\ \psi_-^a \\ \psi_-^b \end{pmatrix}, \quad (1)$$

where the indices a and b refer to the two triangular sublattices of graphene and $+(-)$ to the two Dirac $K(K')$ points. Throughout this paper, we will use the following representation for the Dirac matrices

$$\gamma^0 = \begin{pmatrix} 0 & 1 \\ 1 & 0 \end{pmatrix}, \quad \vec{\gamma} = \begin{pmatrix} 0 & \vec{\sigma} \\ -\vec{\sigma} & 0 \end{pmatrix}, \quad \gamma_5 = \begin{pmatrix} -1 & 0 \\ 0 & 1 \end{pmatrix}; \quad (2)$$

σ^j stand for the Pauli matrices.

The dynamics of the carbon background structure is associated with a charged scalar field φ and with a vector field A_μ . The vacuum expectation value of the scalar field $\langle\varphi\rangle$ vanishes for pure graphene, while for doped or deformed graphene $\langle\varphi\rangle \neq 0$. If $\langle\varphi\rangle \neq 0$, the model generates a fermion mass via spontaneous symmetry breaking.

The lagrangian density for the gauge model reads

$$\begin{aligned} \mathcal{L} = & \bar{\psi} i \gamma^\mu D_\mu \psi - g_2 (\varphi^\dagger \varphi) \bar{\psi} \psi - i h_2 (\varphi^\dagger \varphi) \bar{\psi} \gamma_5 \psi \\ & + D^\mu \varphi^\dagger D_\mu \varphi - V(\varphi^\dagger \varphi) \\ & - \frac{1}{4} F^{\mu\nu} F_{\mu\nu}, \end{aligned} \quad (3)$$

where the fermionic covariant derivative is $D_\mu = \partial_\mu + igA_\mu$, with a similar expression for the bosonic covariant derivative after replacing g by g_φ ,

$$V(\varphi^\dagger \varphi) = \mu^2 (\varphi^\dagger \varphi) + \frac{\lambda_4}{2} (\varphi^\dagger \varphi)^2 + \frac{\lambda_6}{3} (\varphi^\dagger \varphi)^3 \quad (4)$$

up to a constant V_0 , and

$$F_{\mu\nu} = \partial_\mu A_\nu - \partial_\nu A_\mu \quad (5)$$

is the usual Maxwell tensor for the vector bosonic field.

In what concerns the electrons and its interactions with φ and A_μ , the lagrangian (3) is a particular case of the possible theories studied in⁹. In the following, we will consider only the solitonic solutions of the scalar field equation of motion. The lagrangian (3) is an example of fermionic dynamics.

In (4), the coupling constants μ^2 , λ_4 , λ_6 parametrize the self-couplings of the carbon structure and are associated with the carbon mechanical properties like phonon masses, phonon self-interactions and graphene stiffness.

The lagrangian density (3) is invariant under local $U_f(1) \otimes U_b(1)$ transformations. Recall that $\varphi^\dagger \varphi$ can be identified with a dynamical fermionic mass that is a function of space and time. Given that for doped graphene $\langle\varphi\rangle \neq 0$, this term generates a fermionic mass gap, which vanishes for the ground state of pure graphene. Besides the generating of a mass term for the fermions, the model also gives masses for the scalar and vector degrees of freedom. The model allows for vortex solutions for the pure bosonic sector of the theory.

One of the goals of the present work is to investigate how the bosonic degrees of freedom in (3) can be excited via the coupling with an external electromagnetic field C_μ . The coupling with C_μ is introduced in the usual way, i.e. via the minimal prescription, where a ieC_μ should be added to the covariant derivative, where e stands for a generic electric charge.

A. Equations of Motion

The equations of motion associated with the various fields are derived from \mathcal{L} in the usual way. For fermions, they are given by

$$\left\{ i\gamma^\mu D_\mu - (g_2 + ih_2 \gamma_5) (\varphi^\dagger \varphi) \right\} \psi = 0, \quad (6)$$

where $D_\mu = \partial_\mu + igA_\mu + ieC_\mu$ is the covariant derivative. The corresponding equation for the scalar field φ is

$$\begin{aligned} D^\mu D_\mu \varphi = & -g_2 \varphi \bar{\psi} \psi - ih_2 \varphi \bar{\psi} \gamma_5 \psi \\ & - \left\{ \left(\mu^2 + e_\varphi^2 (C^z)^2 \right) \right. \\ & \left. + \lambda_4 (\varphi^\dagger \varphi) + \lambda_6 (\varphi^\dagger \varphi)^2 \right\} \varphi \end{aligned} \quad (7)$$

with the covariant derivative being $D_\mu = \partial_\mu + ig_\varphi A_\mu + ie_\varphi C_\mu$ and e_φ being the effective electric charge of φ . The

gauge field equation of motion reads

$$\partial_\mu F^{\nu\mu} = -g \bar{\psi} \gamma^\nu \psi - i g_\varphi \varphi^\dagger (D^\nu \varphi) + i g_\varphi (D^\nu \varphi)^\dagger \varphi. \quad (8)$$

In what concerns the coupling with the external electromagnetic field C_μ , the lagrangian density and the equations of motion show that, to lowest order in perturbation theory, the coupling with φ is of order e_φ , while A_μ is of the order $g_\varphi e_\varphi$ or e_φ^2 . Then, one expects the degrees of freedom associated with φ to have a high probability of being excited through the incidence of an electromagnetic wave.

B. Hamiltonian Density

The Hamiltonian density \mathcal{H} can be read from the energy-momentum tensor

$$T^{\mu\nu} = \sum_{u=\bar{\psi},\psi,\varphi^\dagger,\varphi,A_\mu} \frac{\partial \mathcal{L}}{\partial (\partial_\mu u)} \partial^\nu u - g^{\mu\nu} \mathcal{L}. \quad (9)$$

It follows that

$$\begin{aligned} \mathcal{H} = T^{00} = & -i\bar{\psi} \vec{\gamma} \cdot (\nabla - ig\vec{A} - ie\vec{C}) \psi + \bar{\psi} \gamma^0 (gA^0 + eC^0) \psi + g_2 (\varphi^\dagger \varphi) \bar{\psi} \psi + ih_2 (\varphi^\dagger \varphi) \bar{\psi} \gamma_5 \psi \\ & + \pi^\dagger \pi + \vec{D}\varphi^\dagger \cdot \vec{D}\varphi + V(\varphi^\dagger \varphi) + \frac{1}{2} (\vec{E}^2 + \vec{B}^2) \end{aligned} \quad (10)$$

where $\pi^\dagger = \partial^0 \varphi$ and $\pi = \partial^0 \varphi^\dagger$ are the canonical momentum density fields associate with φ and φ^\dagger , respectively. The vectors \vec{E} and \vec{B} are the usual electric and magnetic fields associated with the gauge vector A_μ .

III. SOLITON-LIKE SOLUTIONS FOR GRAPHENE AND NANOTUBES

In this section we will discuss the solutions of classical equations of motion. Let us for the moment disregard the contributions coming from fermions and gauge fields. The model assumes that the scalar and vector fields are associated with the carbon lattice background. The Dirac electrons are soft degrees of freedom and one expects that the fermion-scalar couplings are subleading for the dynamics of the scalar field.

Assuming that the only dynamical field is φ , the corresponding classical configurations are obtained solving equation (7). In order to compute solitonic like solutions,

we will consider the following ansatz

$$\varphi(\vec{r}, t) = \phi(x - vt) e^{iky} \quad (11)$$

for a graphene sheet living on the xy -plane and

$$\varphi(\vec{r}, t) = \phi(z - vt) e^{in\theta}, \quad (12)$$

for a nanotube whose symmetry axis is the z -axis. In order to describe the nanotube we use cylindrical coordinates r , θ and z .

The ansatz (11) and (12) reduce the partial differential equation (7) to an ordinary differential equation in the variable ζ , where

$$\zeta = \begin{cases} x - vt, & \text{for graphene,} \\ z - vt, & \text{for a nanotube.} \end{cases} \quad (13)$$

In terms of ζ , equation (7) becomes

$$(1 - v^2)\phi'' = (\mu^2 + k^2)\phi + \lambda_4 \phi^3 + \lambda_6 \phi^5, \quad (14)$$

where a prime means a derivative with respect to ζ .

The ansatz (12) used to describe nanotubes, makes the equation of motion equal to (14) after the replacement of k^2 by n^2/R^2 . In the following, we will explore the solutions of equation (14) for graphene, but one should

have in mind that the results for graphene have a directly translation into nanotubes.

The energy associated with the solitonic waves (11) is given by

$$E_{graph} = W \int_{-L_x/2}^{L_x/2} dx \left\{ (1+v^2)(\phi')^2 + (\mu^2 + k^2)\phi^2 + \frac{1}{2}\lambda_4\phi^4 + \frac{1}{3}\lambda_6\phi^6 \right\}, \quad (15)$$

where L_x and W are the dimensions of the graphene sheet. For a nanotube of radius R and length L , the energy associated with the non-linear wave (12) is given by (15) after the replacement of W by $2\pi R$ and of k^2 by n^2/R^2 . For graphene and nanotubes the lowest energy state is associate with $v = 0$, i.e. for a static solution, and with $k = 0$ for graphene or $n = 0$ for nanotubes. Furthermore, for the static solution, i.e. when $v = 0$, minimizing the energy is equivalent to solve the classical equation motion (14).

From the point of view of the differential equation (14), the solutions describing travelling solitonic waves, i.e. for solutions with $v \neq 0$, are the static solutions after the rescaling of the potential parameters $\mu^2 + k^2$, λ_4 and λ_6 by the inverse of $1 - v^2$. Note that for $v < v_f \approx c/300$ the rescaling does not change the nature of the solution derived for $v = 0$. However, for $v > v_f$ the rescaling formally changes the sign of coupling constants and can lead to a change on the functional form of the solution. Given that we aim to investigate non-linear waves associated with the carbon structure of graphene and nanotubes, one expects to be closer to the first case, $v < v_f$, and we will not explore the situation where the solitonic wave moves faster than the fermions $v > v_f$. From now on, we will assume that $v = 0$ except where stated explicitly.

Before starting to discuss the solutions of the equation of motion (14), let us define the notation. In the following, the k^2 term will be included in the definition of the potential, i.e. we will write

$$V(\phi) = (\mu^2 + k^2)\phi^2 + \frac{1}{2}\lambda_4\phi^4 + \frac{1}{3}\lambda_6\phi^6. \quad (16)$$

Then, the energy becomes

$$\begin{aligned} E &= W \int_{-L_x/2}^{L_x/2} dx \left\{ (\phi')^2 + V(\phi) \right\} \\ &= 2W \int_{-L_x/2}^{L_x/2} dx V(\phi), \end{aligned} \quad (17)$$

where to write the last expression we have used the equation of motion.

1. Kink Solution

An analytical solution for (14) can be obtained when $\lambda_6 = 0$ and

$$V(\phi) = \frac{\lambda_4}{2}(\phi^2 - \phi_0^2)^2. \quad (18)$$

Note that a constant $V_0 = \lambda_4\phi_0^4/2$ was added to the original potential $V(\phi)$ in order to have a positive defined potential energy. In terms of the original potential one has $\lambda_6 = 0$ and $\mu^2 + k^2 = -\lambda_4\phi_0^2$. The classical configurations are

$$\phi(\zeta) = \pm \phi_0 \tanh \left\{ \phi_0 \sqrt{\frac{\lambda_4}{2}} (\zeta - \zeta_0) \right\}, \quad (19)$$

where ζ_0 is a constant of integration. The plus (minus) sign solution is known in the literature as kink (antikink). For an infinite length sheet of graphene, the energy associated with (19) is given by

$$E_{sol} = \frac{4}{3} \sqrt{2\lambda_4} \phi_0^3 W. \quad (20)$$

2. A Solution for a ϕ^6 Potential

The classical configuration associated with the potential energy

$$V(\phi) = \frac{\lambda^2}{2}\phi^2(\phi^2 - \phi_0^2)^2, \quad \lambda > 0 \quad (21)$$

was investigated by Lohe in¹². The constants in the original potential are given by $\lambda_6 = 3\lambda^2/2$, $\lambda_4 = -2\lambda^2\phi_0^2$ and $\mu^2 + k^2 = \lambda^2\phi_0^4/2$. The equations of motion have the solutions

$$\phi(\zeta) = \pm \frac{\phi_0}{\sqrt{2}} \sqrt{1 \pm \tanh \left[\frac{\lambda\phi_0^2}{\sqrt{2}} (\zeta - \zeta_0) \right]}. \quad (22)$$

The energy associated with any of these configurations is given by

$$E_{sol} = \frac{\sqrt{2}}{8} \lambda^2 \phi_0^4 W \quad (23)$$

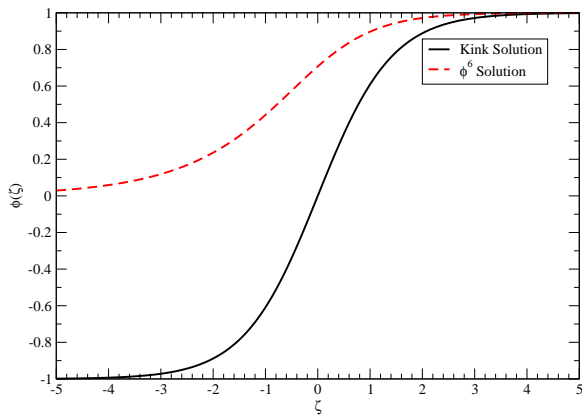


FIG. 1: The solutions (19) and (22) in arbitrary units. All constants where set to one and $\zeta_0 = 0$.

for a graphene with infinite length and for any combination of plus and minus signs.

The profile of solutions (19) and (22) can be seen in figure 1.

A. Energy Estimation

The system of units used so far take $\hbar = 1$ and the Fermi velocity $v_F = 1$. In order to convert to the usual system of units, we will use for the speed of light $c = 2.998 \times 10^8$ m/s, $v_F = c/300$ and $\hbar v_F = 0.6578$ eV nm. To estimate the energy associated with the solitonic configuration, recall that in the gauge model the fermion gap is twice the fermion mass, i.e.

$$E_g = 2\sqrt{g_2^2 + h_2^2} \phi_0^2; \quad (24)$$

see⁹ for details. For nanoribbons, a typical value for the gap¹³ being 0.1 eV for $W = 10$ nm. For $\sqrt{g_2^2 + h_2^2} \approx 1$, it follows that

$$\phi_0^2 = 0.05 \text{ eV} \quad (25)$$

and

$$E_{sol} = \left(0.23 \text{ eV}^{1/2}\right) \sqrt{\lambda_4} \left(\frac{W}{10 \text{ nm}}\right), \quad (26)$$

for the kink solution discussed in section III 1, where λ_4 is given in eV and the width W in nm, and

$$E_{sol} = \left(6.7 \text{ meV}\right) \lambda^2 \left(\frac{W}{10 \text{ nm}}\right) \quad (27)$$

for the soliton of section III 2; recall that λ is dimensionless. Note that according to (20) and (23) (24), the energy associated with the solitonic configurations is driven by the mass gap. Furthermore, from (19) and (22) one can estimate the dimension l of the transition region associated with each of the solitonic solution. Indeed, from $\phi_0^2 = 0.05$ eV it follows for the kink solution

$l \approx 2/\phi_0 \sqrt{\lambda_4} = 14/\sqrt{\lambda_4}$ nm, for λ_4 given in eV. For the other nonlinear wave $l \approx \sqrt{2}/\lambda \phi_0^2 = 43/\lambda$ nm.

In order to understand how the energy of the non-linear wave changes with W , one has to consider $E_g(W)$. In¹⁶ $E_g(W)$ was investigated experimentally and the authors conclude that for $W > 16$ nm, the observed gaps are well described by

$$E_g(W) = \frac{\alpha}{W - W^*}, \quad (28)$$

where $\alpha = 0.2$ eV nm and $W^* = 16$ nm. Taking into account $E_g(W)$, it follows that the energy of the solitonic solutions behave as

$$E \propto \frac{W}{(W - W^*)^{3/2}} \quad \text{and} \quad \frac{W}{(W - W^*)^2}, \quad (29)$$

where the first result is for the kink solution (see section III 1) and the later for the solutions of section III 2. In both cases E vanish in the limit of infinite width, i.e. when graphene is recovered. This result opens the possibility of tuning the energy of the nonlinear modes by chosen the nanoribbon width.

From the point of view of exciting these nonlinear modes of the carbon honeycomb structure, the results summarized in equation (29) mean that as graphene becomes wider, it will be to easier to excite the solitonic modes. In particular for bulk graphene these solitonic modes have zero energy and they must be a component of the graphene ground state wave function.

As a side remark, we would like to point out that as the width becomes sufficiently small, the edges of the carbon structure, being zig-zag or armchair-shaped, should be taken in the computation of the solitonic energy.

IV. COUPLING ELECTROMAGNETIC AND THE NONLINEAR WAVES

The soliton modes are associated with a complex scalar field φ and, therefore, they couple with the electromagnetic field C_μ through and effective electric charge e_{sol} . The Hamiltonian describing the interaction between φ and C_μ is given by

$$H_I = \int dx dy \left\{ ie_{sol} C^\mu [(\partial_\mu \varphi^\dagger) \varphi - \varphi^\dagger (\partial_\mu \varphi)] + e_{sol}^2 C_\mu C^\mu (\varphi^\dagger \varphi) \right\}. \quad (30)$$

For a classical scalar field, to describe either photon absorption or emission, one has to evaluate the matrix element of H_I between the one photon state $|\vec{\epsilon}, \vec{q}\rangle$ with energy $E_\gamma = |\vec{q}|$ and polarization $\vec{\epsilon}$ and the electromagnetic vacuum. The decay rate of the classical nonlinear mode is controlled by the following matrix element, computed in the limit of long wavelengths,

$$\langle \vec{\epsilon}, \vec{q} | H_I | 0 \rangle = 2 \sqrt{\frac{2\pi c}{q}} e_{sol} k \int dx dy \phi(x) \phi'(x) (\vec{\epsilon} \cdot \hat{e}_y), \quad (31)$$

up to a volume normalization associated with the photon state. In (31) c stands for the velocity of light in the vacuum and \hat{e}_y is the unit vector along y direction.

Equation (31) shows that only electromagnetic waves polarized along the y direction, i.e. for a photon polarization along the shortest direction of the graphene sheet, are able to couple to the solitonic modes. For nanotubes, \hat{e}_y is replaced by \hat{e}_θ , the unit vector along the θ direction, and the photon polarization needs an \hat{e}_θ component in order to couple to the solitonic modes.

For the kink solution (section III 1) the integrand function in (31) is antisymmetric and the matrix element vanishes. In the long wavelength limit, the kink solutions do not couple to the photon.

For the non-linear solution of the equations of motion discussed in section III 2, it follows that

$$\langle \vec{\epsilon}, \vec{q} | H_I | 0 \rangle = 2 \sqrt{\frac{2\pi c}{q}} e_{sol} k \phi_0^2 (\vec{\epsilon} \cdot \hat{e}_y) W. \quad (32)$$

It follows that the decay rate for photon production grows with the width squared and ϕ_0^4 , i.e. the fermionic mass gap squared. For the configuration (22), it follows that, see equation (24),

$$|\langle \vec{\epsilon}, \vec{q} | H_I | 0 \rangle|^2 = 2\pi c e_{sol}^2 \frac{k^2}{q} (\vec{\epsilon} \cdot \hat{e}_y)^2 \frac{W^2 E_g^2}{g_2^2 + \hbar_2^2} \quad (33)$$

A non-vanishing matrix element requires not only a photon polarized along the shortest direction of the graphene sheet but also a solitonic wave which transport momenta k along the y direction.

In what concerns the scaling of the transition rate Γ with W , combining equations (29) and (33), it follows that for $W > 16$ nm

$$\Gamma \propto \left(\frac{W}{W - W^*} \right)^4. \quad (34)$$

V. CONCLUSIONS

The gauge model for graphene suggested in⁸ and extended in⁹, combined with the phenomenological observation of how the mass gap changes with the graphene width, predicts that solitonic waves can couple to the electromagnetic field, provided the photon has the right polarization. The decay rate is non-vanishing only when the photon polarization has a component along the y direction for graphene or along the θ direction for a nanotube.

From the point of view of the mass gap, the non-linear waves can be thought as giving rise to regions in graphene where the electrons behave as massless particles, those where $\phi \sim 0$, and regions where the electrons acquire a finite mass, regions where $\phi \sim \phi_0$. If experimentally one can distinguish such regions by means of a spectroscopic analysis like, for example, scanning tunneling microscope as performed in¹⁴ for the different graphene terminations

or in¹⁵ to investigate one dimensional defects, then one could observe directly the mass profiles and extract information on the solitonic waves, provided that the life time of these non-linear states is long enough. From these profiles one can constraint the possible forms of the scalar potential $V(\phi)$ and, in this way, help to better define the effective model.

The problem discussed here has several energy scales which behave differently with W . This different scaling can, in principle, be explored to identify the soliton modes of section III 2. As discussed above, $E_g \propto \phi_0^2$. Therefore, the energy associated with the soliton scales as

$$E_{sol} \propto E_g^{3/2} W \quad \text{and} \quad E_g^2 W \quad (35)$$

for the kink solution (19) and for (22), respectively. This result suggests that the energy of the solitonic modes scales with mass gap E_g to a given power and the nanoribbon width.

This different behavior can be explored, in a systematic investigation of the spectra of photon emission with W , to identify the nonlinear modes in graphene nanoribbons and improve our understanding of the effective theory discussed here.

In what concerns the typical energy associated with the solitonic modes, the estimates performed at the end of section III A suggests, for example, $E_{sol} \sim 7$ meV for a $W \sim 10$ nm for the case of an effective potential which goes as φ^6 . Then, the possible transitions involving the nonlinear modes open a window to explore the far infrared and terahertz frequencies. Furthermore, the coupling of the nonlinear waves with the electromagnetic field are sensible to the photon polarization. The nanoribbon is transparent to photons polarized along the largest length, but not to those polarized along the nanoribbon width. These characteristics are of interest for optical devices as, for example, broadband polarizers applied to photonics circuits for telecommunications. Note, however, that similar properties can occur in association with electronic intraband transitions as described in¹⁷. A possible way to distinguish between the two mechanism is to investigate the behavior with the chemical potential. For the solitons, the results described here are independent of the chemical potential. Dichroism with intraband transitions requires a non-vanishing chemical potential.

We believe that our discussion can motivate experiments that could disentangle and identify the role of the carbon structure via the presence of nonlinear waves and/or intraband electronic transitions in graphene nanoribbons.

Acknowledgements

We thank A. J. Chaves for useful discussions and comments. The authors acknowledge financial support from the Brazilian agencies FAPESP (Fundação de Amparo à

Pesquisa do Estado de São Paulo) and CNPq (Conselho Nacional de Desenvolvimento Científico e Tecnológico). O. Oliveira acknowledges financial support from FCT

under contracts PTDC/FIS/100968/2008 under the initiative QREN financed by the UE/FEDER through the Programme COMPETE.

-
- ¹ P. R. Wallace, *Phys. Rev.* **71**, 622 (1947).
² K. S. Novoselov, A. K. Geim, S. V. Morozov, D. Jiang, Y. Zhang, S. V. Dubonos, I. V. Gregorieva, A. A. Firsov, *Science* **306**, 666 (2004).
³ D. S. L. Abergel, A. Russell, V. I. Falko, *Appl. Phys. Lett.* **91**, 063125 (2007).
⁴ P. Blake, K. S. Novoselov, A. H. Castro Neto, D. Jiang, R. Yang, T. J. Booth, A. K. Geim, E. W. Hill, *Appl. Phys. Lett.* **91**, 063124 (2007).
⁵ C. Casiraghi, A. Hartschuh, E. Lidorikis, H. Qian, H. Harutyunyan, T. Gokus, K. S. Novoselov, A. C. Ferrari, *Nano Lett.* **7**, 2711 (2007).
⁶ A. H. Castro Neto, F. Guinea, N. M. R. Peres, K. S. Novoselov and A. K. Geim, *Rev. Mod. Phys.* **81**, 109 (2009).
⁷ N. M. R. Peres, *Rev. Mod. Phys.* **82**, 2673 (2010).
⁸ R. Jackiw, S.-Y. Pi, *Phys. Rev. Lett.* **98**, 266402 (2007).
⁹ O. Oliveira, C. E. Cordeiro, A. Delfino, W. de Paula, T. Frederico, *Phys. Rev.* **B 83**, 155419 (2011).
¹⁰ R. Jackiw, A. I. Milstein, S.-Y. Pi, I. S. Terekhov, *Phys. Rev. B* **80**, 033413 (2009).
¹¹ R. Jackiw, *Physics Today* **25**, 23 (1972).
¹² M. A. Lohe, *Phys. Rev.* **D 20**, 3120 (1979).
¹³ X. Li, X. Wang, L. Zhang, S. Lee, H. Dai, *Science* **319** 1229 (2008).
¹⁴ Y. Kobayashi, K.-i. Fukui, T. Enoki, K. Kusakabe, Y. Kaburagi, *Phys. Rev.* **B 71**, 193406 (2005).
¹⁵ J. Lahiri, Y. Lin, P. Bozkurt, I. I. Oleynik, M. Batzill, *Nat Nanotechnol* **5**, 326 (2010).
¹⁶ M. Y. Han, B. Özyilmaz, Y. Zhang, P. Kim, *Phys. Rev. Lett.* **98**, 206805 (2007).
¹⁷ F. Hipolito, A. J. Chaves, R. M. Ribeiro, M. I. Vasilevskiy, V. M. Pereira, N. M. R. Peres, *Phys. Rev.* **B86** 115430 (2012).